Crystal Structure of Native Chicken Fibrinogen at 2.7 Å Resolution[†,‡]

Zhe Yang, Justin M. Kollman, Leela Pandi, and Russell F. Doolittle*

Center for Molecular Genetics, University of California, San Diego, La Jolla, California 92093-0634

Received July 3, 2001; Revised Manuscript Received August 15, 2001

ABSTRACT: The crystal structure of native chicken fibrinogen (320 kDa) complexed with two synthetic peptides has been determined at a resolution of 2.7 Å. The structure provides the first atomic-resolution view of the polypeptide chain arrangement in the central domain where the two halves of the molecule are joined, as well as of a putative thrombin-binding site. The amino-terminal segments of the α and β chains, including fibrinopeptides A and B, are not visible in electron density maps, however, and must be highly disordered. The αC domain is also very disordered. A residue by residue analysis of the coiled coils with regard to temperature factor shows a strong correlation between mobility and plasmin attack sites. It is concluded that structural flexibility is an inherent feature of fibrinogen that plays a key role in both its conversion to fibrin and its subsequent destruction by plasmin.

Fibrinogen is the large hexameric ($\alpha_2\beta_2\gamma_2$) glycoprotein found in the blood plasma of all vertebrate animals that is the precursor to fibrin clots. Its molecular mass varies from 320 to 400 kDa depending on the species of origin, the variations invariably being due to differences in the carboxyl-terminal region of the α chains (*1*). The conversion to fibrin is effected by the thrombin-catalyzed removal of peptides ("fibrinopeptides") from the amino-terminal regions of the α and β chains, the exposure of "knobs" that fit into "holes" on companion molecules being at the heart of the polymerization. During this process, the growing protofibrils are covalently cross-linked by the thrombin-activated transglutaminase, factor XIII. Eventually, fibrin is destroyed by a proteolytic cascade which is in part activated by fibrin itself.

Shadow-cast electron microscope images of fibrinogen long ago revealed a triglobular structure approximately 470 Å in length (*2*), giving credence to many other experiments that implied the molecule contained both globular and extended regions, including α-helical "coiled coils" (*3*). The domainal nature of the globular parts of the molecule was further delimited by negative staining electron microscopy and low-resolution X-ray crystallography (*4*, *5*). In recent years, X-ray structures of some core fragments have been determined, including a 30 kDa recombinant protein corresponding to the carboxyl-terminal domain of the γ chain of human fibrinogen (*6*, *7*) and the 86 kDa fragment D from human fibrinogen and its cross-linked equivalent from fibrin (*8*−*10*). The D fragments account for about half the mass of the fibrinogen molecule. The partial structure of a 285 kDa moiety prepared by limited proteolysis of bovine fibrinogen has also been reported at an approximate resolution of 4 Å (*11*).

Until very recently, there were no reports of X-ray quality crystals for a native fibrinogen. One of the challenges in obtaining such crystals is the apparent mobility of the carboxyl domains of the α chains. These 25−35 kDa domains ("αC") are the most variable parts of the molecule on a species to species basis (*1*, *12*). They are easily trimmed away by many different proteases and are often termed "free-swimming appendages" (*1*). Moreover, most contain a series of repeated sequences (*12*, *13*) that likely add to the flexible nature of the region. As it happens, chicken fibrinogen α chains lack these repeats (*14*), an attribute that led us to undertake crystallization of that protein. Crystals were in fact obtained, and a low-resolution structure was determined (*15*).

The early work with crystals of chicken fibrinogen was problematic in that the crystals diffracted anisotropically and did not freeze well; results were limited to data collected at room temperature, including crystals that were stabilized with glutaraldehyde (*15*). Since then, however, we have found a new crystallizing agent and determined suitable conditions for freezing. These two advances have yielded crystals that diffract to 2.7 Å resolution. Not surprisingly, some of the features of the low-resolution model have had to be modified in light of the high-resolution structure. Some discrepancies were also apparent between the new X-ray structure and amino acid sequences previously reported for chicken fibrinogen, leading us to conduct DNA sequencing on certain regions. Two errors were found: a glycine at α48 in the first disulfide ring that had been reported as a cysteine and an alanine at γ chain residue 286 that had been thought to be an arginine (unless otherwise stated, human fibrinogen numbering is used throughout this article).

MATERIALS AND METHODS

Trimethylamine oxide (TMAO) and methylpentanediol (MPD) were obtained from Aldrich. Peptides corresponding to fibrin amino-terminal sequences were synthesized by the BOC procedure on a Beckman model 990 synthesizer.

[†] This work was supported by Grant HL-26873 from the National Heart, Lung and Blood Institute. J.M.K. was supported by NIH Training Grant GM 007240.

[‡] The atomic coordinates for this structure have been deposited in the Protein Data Bank (entry 1JFE).

* To whom correspondence should be addressed: Center for Molecular Genetics, Rm. 206, University of California, San Diego, La Jolla, CA 92093-0634. Telephone: (858) 534-4417. Fax: (858) 534-4985. E-mail: rdoolittle@ucsd.edu.

10.1021/bi011394p CCC: $20.00
Published on Web 09/28/2001

Chicken Fibrinogen. Fresh blood was collected at Wing Lee Poultry (San Diego, CA) into approximately $^1/_{10}$ volume of cold 0.1 M trisodium citrate and centrifuged to remove cells. Crude fibrinogen was prepared by a modified cold ethanol method, after which the preparation was passed first over a Gly-Pro-Arg-Pro affinity column (*16*) and then lysine-Sepharose (*17*). The material was concentrated to 6 mg/mL in 0.15 M NaCl and 0.05 M imidazole (pH 7.0) and stored in small aliquots at −70 °C. Unreduced preparations gave single bands upon SDS gel electrophoresis. Amino-terminal sequencing (University of California, San Diego, Sequencing Facility) gave a single amino-terminal sequence (YIATREN), both the α and β chains being blocked by cyclized terminal glutamines. The quality of the fibrinogen during crystallization was continuously monitored on aliquots from neighboring drops up to and after the irradiation of the crystals.

Crystallization. Crystals were obtained by vapor diffusion from sitting drops at room temperature. Trimethylamine oxide (TMAO), which is known to stabilize proteins (*18*), was used as a precipitant. Synthetic peptide ligands corresponding to the A and B knobs (*19*) were added to the protein solution before the addition of the precipitant. Thus, fibrinogen solutions [6 mg/mL in 0.15 M NaCl and 0.05 M imidazole (pH 7.0)] containing 2 mM GPRPam[1] and GHRPam were mixed volume for volume with well solutions containing 0.5 M TMAO, 0.05 M MES (pH 6.0), 1 mM $CaCl_2$, and 1 mM sodium azide. Crystals suitable for X-ray diffraction grow over the course of 1−2 weeks.

Data Collection and Processing. Diffraction data were collected at the Advanced Light Source (beamline 5.0.2). Crystals were graded into 20% methylpentanediol (MPD) and flash-frozen at 100 K. Data processing with Denzo and Scalepack (*20*) confirmed that the crystals belong to space group $P2_1$ (Table 1). There is one molecule in the asymmetric unit; the solvent content is approximately 65%.

Structure Determination. Molecular replacement was carried out with AMORE (*21*, *22*) in the resolution range of 10−4 Å. A single D domain from a 2.3 Å structure of cross-linked fragment D (PDB entry 1FZC) was used as a search model. Residues of human fragment D that differ from the chicken sequence were replaced with alanines or, where appropriate, glycines. A solution was found that corresponded to the two D fragments in each fibrinogen molecule. The correlation coefficient was 34.1 and the *R*-factor 0.475. Initial $2F_o - F_c$ and $F_o - F_c$ difference electron density maps were calculated at 2.7 Å using the fragment D phases with SIGMAA weighting (*23*). The earlier 5.5 Å model (*15*), which encompassed the full extent of the interdomainal coiled coils and the connections within the central domain, was used as a preliminary guide to model building with the program package O (*24*). Refinement was accomplished with the CNS package (*25*), including the slow-cool protocol and group and individual *B*-factor refinements. Numerous cycles of refining and rebuilding were conducted. Loose noncrystallographic restraints were imposed on the βC, γC, and central domains of the dimer throughout the refinement process.

[1] Abbreviations: GPRPam, Gly-Pro-Arg-Pro-amide; GHRPam, Gly-His-Arg-Pro-amide; TMAO, trimethylamine oxide; MPD, methylpentanediol; LSQ, least-squares; rms, root-mean-square; PCR, polymerase chain reaction; MES, morpholinoethane sulfonate.

Table 1: Data Collection and Refinement Statistics

space group	$P2_1$
unit cell dimensions	$a = 114.1$ Å, $b = 100.0$ Å, $c = 200.1$ Å, $\beta = 105.8°$
no. of molecules per asymmetric unit	1
no. of crystals	1
highest resolution (Å)	2.65
no. of observations	1506048
no. of unique reflections	121776
completeness (%)	94.8
completeness in the highest-resolution shell (2.74−2.65 Å) (%)	67.8
R_{sym} (I) (%)[a]	8.4
mosaicity	0.6
% solvent	63.4
Matthews coefficient	3.43
refinement resolution range (Å)	20.0−2.7
no. of residues in protein	2728
no. of residues in model	1959 (71.8%)
R-factor[b]	0.227
R_{free}[c]	0.255
rmsds from ideal values	
bond lengths (Å)	0.007
bond angles (deg)	1.3

[a] $R_{sym} = (\sum|I - \langle I\rangle|)/(\sum|I|)$. [b] Crystallographic *R*-factor $[(\sum||F_{obs}| - |F_{calcd}||)/(\sum|F_{obs}|)]$ with 95% of the native data for refinement. [c] R_{free} is the *R*-factor based on 5% of the native data withheld from refinement.

Model Depiction. Illustrations involving the model structure were prepared with various rendering programs, including XtalView (*26*), Molscript (*27*), Raster 3D (*28*), Conscript (*29*), Grasp (*30*), and Ribbon (*31*).

DNA Sequencing. During the analysis of the data, it became clear that there were two positions where the diffraction data were not in agreement with the reported amino acid sequence for chicken fibrinogen. Accordingly, we purchased chicken genomic DNA (Novagen) and the appropriate oligonucleotide primers (Operon) and used PCR to isolate the relevant regions. Sequencing (GenBase) revealed that chicken α chain residue 48 is glycine and not cysteine as originally reported (*14*). Additionally, γ chain residue 286 is alanine and not arginine.

RESULTS

The mainframe structure of chicken fibrinogen, not including the flexible αC domains, is sigmoidal in shape (Figure 1), the plane of the "S" being normal to an approximate 2-fold axis. The molecule measures 460 Å in its longest dimension and ∼65 Å in the plane of the S. As was apparent from lower-resolution studies (*11*, *15*), the structure bears a strong resemblance to images obtained by negative staining electron microscopy (*4*). Two sets of three-stranded coiled coils connect the distal globular regions (D fragments) and meet at the abutting disulfide rings in the center of the molecule. The disordered αC domains reside in the sinuses of the coiled coils mostly away from the central domain (Figure 2).

The molecule possesses a dorsal−ventral aspect across the sigmoidal plane, the centrally located γ chain amino termini residing on what we have designated the dorsal side, and the amino-terminal segments of the α and β chains, to the extent that they can be visualized, being on the ventral side. A similar situation exists at the extremities of the molecule

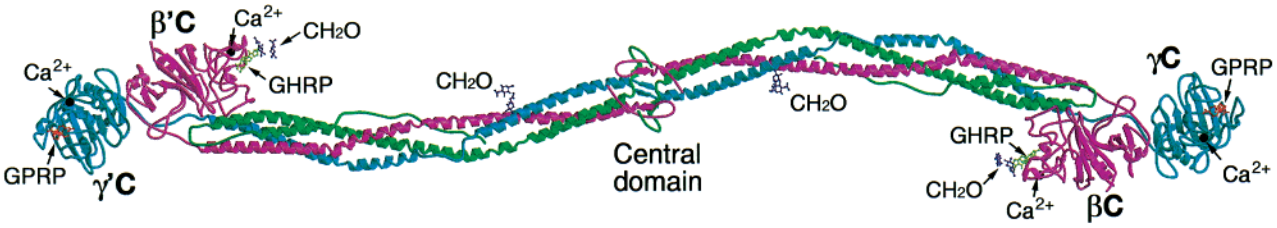

FIGURE 1: Ribbon model of chicken fibrinogen showing distal globular domains connected by three-stranded coiled coils that meet at a central focus and other features of the molecule (α chains, green; *β* chains, magenta; *γ* chains, blue).

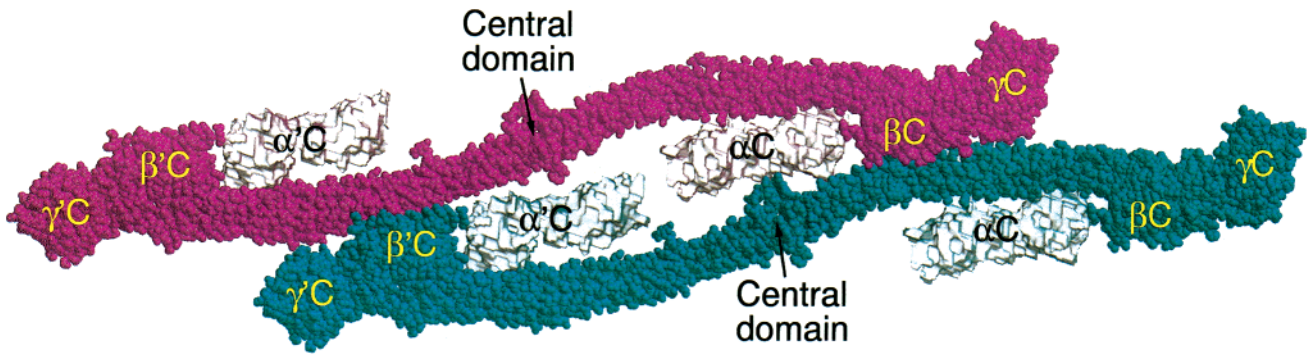

FIGURE 2: Space-filling representation including disordered αC domains (light colored netting). The ordered parts of two neighboring molecules are colored magenta and blue, respectively.

where the *γ* chain holes into which the A knobs must fit are diametrically opposite the *γ* chain cross-linking sites (*8*).

Certain parts of the protein remain elusive. Electron density maps barely reveal the outlines of the disordered carboxyl regions of the α chains (Figure 2), and the amino-terminal segments of the α and *β* chains, including fibrinopeptides A and B, could not be resolved. The reasonable *R*-factors found after refinement (Table 1) indicate that these parts of the molecule do not contribute significantly to the diffraction and must be highly disordered. That the missing portions had not been lost to degradation during incubations leading to crystallization was ascertained by SDS gels and amino-terminal sequencing. The mobility implied by the unresolved portions of the protein is testimony to flexibility being a functional attribute of fibrinogen.

Central Domain and Disulfide Rings. The two central disulfide rings appear as prominent doughnuts of density (Figure 3). As was shown in the low-resolution model (*15*), the connections within each ring involve junctions between cysteines *β*76 and α49, α45 and *γ*23, and *γ*19 and *β*80. The X-ray structure for the centrally located disulfide rings shows them to be not as rigid as those in the fragment D region, high *B*-factors implying a more mobile situation. When viewed along an axial projection from either coiled coil, the disulfide rings have a triangular aspect, the amino-terminal segments emerging from the three apexes (Figure 3).

The *γ*Cys19 residues from the two halves of the molecule are opposite each other, and as a result, the comparable α chain Cys45 is opposite the *β* chain Cys76 from the other half of the molecule and vice versa (Figure 3). A series of short antiparallel *β*-strands centered on cysteines α45, *β*76, and *γ*19 hold the abutting disulfide rings in appropriate juxtaposition. The two half-molecules are reciprocally intertwined such that the *γ* chains extend across the central plane and make hydrophobic contact with the coiled coil before turning back to make a "bow tie" at the reciprocal disulfide connection involving residues *γ*Cys9 and *γ*Cys8 (Figure 4).

The *β* chains cross the central plane in a similar manner, in this case forming loops that fit into archways shaped by the opposing α chain segments. The returning *β* chain loop is positioned to form the interchain disulfide bond between its residue *β*65 and α36 from the other half of the dimer before sweeping around the ventral surface of the coiled coil on the side where it originated. The corresponding segments of the α chains barely cross the central plane, at least within the limits in which they could be traced. Instead, they arc around the molecule before meeting on the ventral side where they form a disulfide between the cysteines at α28 diametrically opposite to where the two *γ* chains are bonded (Figure 4).

Taken together with the three short sheets between the disulfide rings, the involvement of the *β* and *γ* chains explains how two half-molecules of fibrinogen find and bind each other before the introduction of the cementing disulfide bonds. The pattern of the disulfide bridging is consistent with previously reported site-directed mutagenesis studies (*32*, *33*).

Coiled Coils. The three-stranded coiled coils are delimited at both ends by interconnected braces of cysteines in all three of the chains called "disulfide rings" (*34*). The two rings bordering the central plane are internally symmetrical in that the first cysteine of a pair in a given chain is bonded to the second of one of the other chains. The disulfide rings in the fragment D region are asymmetric in that the bonding accommodates a reversal of direction by the α chain leading to the formation of the so-called "fourth helix" (*9*).

The electron density through most of the coiled coils region is strong, and most side chains are readily evident. A putative carbohydrate cluster at *γ*Asn52 was obvious, but another at αAsn62 was not. The coiled coils are mostly canonical in the segments nearer to either of the delimiting disulfide rings, the strands loosening up greatly in their

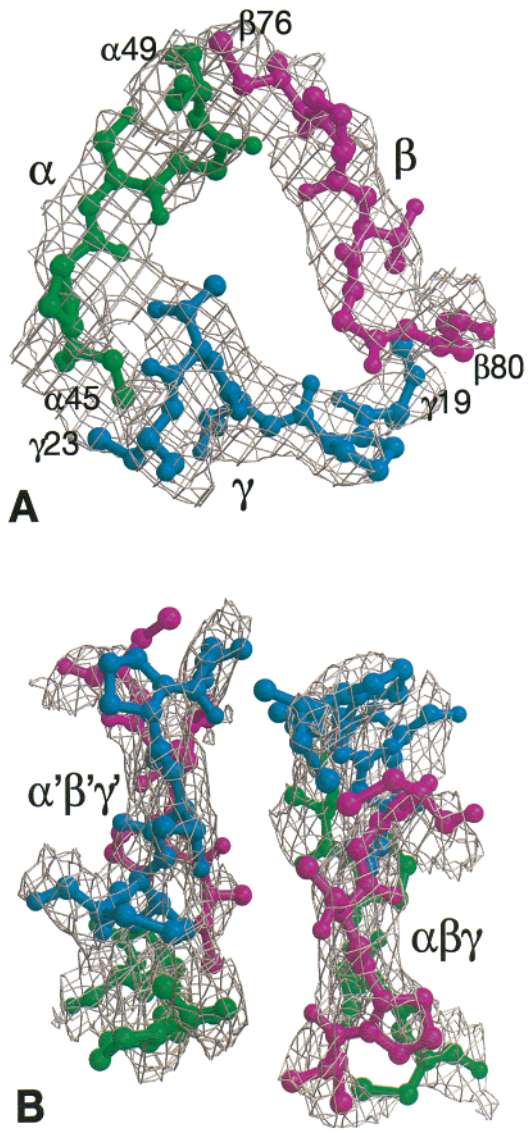

FIGURE 3: Electron density map ($3F_o - 2F_c$) calculated at 1.0σ in regions of the two opposing disulfide rings. The models were not included in the F_c calculations. (A) Ring formed by the A, B, and C chains. (B) Edge views of opposing rings formed by the A, B, and C chains (right) and the D, E, and F chains (left).

central regions as evidenced by *B*-factor (temperature-factor) traces (Figure 5). The high-*B*-factor regions are strongly correlated with known sites of plasmin attack (*35*).

There is a noticeable "bump" in the coiled coil between the proline residues at positions γ69 and γ76. The segment (PSEKQTLP) contains a lysine (γLys72) which, exposed as it is, seems to be a good target for plasmin cleavage. A similar bulge occurs in the bovine structure (*11*), although the lysine in this case is adjacent to a proline (NPDQPSKP) and is unlikely to be able to be cleaved by plasmin. The corresponding human sequence (NPDESSKP) closely resembles that of the bovine.

The end-to-end interactions that occur in the crystal packing of fibrinogen are the same as occur in crystals of D and double-D fragments (*9*). These associations are intrinsically asymmetric (*9*) and require a compensatory twist elsewhere in the fibrinogen molecule in the crystal. Brown et al. (*11*) have reported that in the bovine molecule the coiled coils have "flexible hinges" near their middles. The bovine crystals have two molecules per asymmetric unit, and differences of up to 18° in the bending angles were reported between the two noncrystallographically related molecules. The chicken crystals have only one molecule per asymmetric unit, all molecules having the same crystallographic shape. Structural differences can and should exist between the two halves of the dimeric molecules, however, the consequence of the overall torsional twist caused by end-to-end packing constraints (*15*).

In this regard, the chicken ABC coiled coil can be superimposed on the DEF coiled coil from the other half of the molecule (Figure 6A), even though the unmatched halves of the model are twisted out of line as a result. If only half the lengths of the coiled coils are used for the superposition, then an apparent flex occurs at the position where the superposed residues end (Figure 6B). A similar situation results when the globular γC or βC domains are superimposed on each other (Figure 6C). These results imply that the structural differences between the two halves of the molecule are modest and not focused on a single flex point.

The use of least-squares fitting for superimposing oblong structures is not without its shortcomings. If only sections of a protein are used for the fitting, then small differences in orientation will accumulate and the remaining parts of the molecule will necessarily veer away. Nonetheless, after examining the superposition of many different segments of the chicken model, we conclude that the twist in the nonhelical central portions of the coiled coils is significantly more pronounced than in the helical regions. Because end-to-end packing in fibrin is the same as in the crystal (*9*), it is possible that these torsional adjustments contribute to fibrinogen and fibrin being recognized differently by other macromolecules.

Flexible αC Domains. The X-ray structure of fragment D from human fibrinogen revealed that the α chain makes an abrupt reversal within the distal disulfide ring, the returning chain forming a fourth helix running in the opposite direction with respect to the three-stranded coil (*8*). In the chicken structure, the returning α chain (fourth helix) stretches from residue α164 to approximately residue α220 before the electron density becomes too loose to follow with confidence. In neither half of the dimeric structure is the segment helical over its entire course, the *B*-factor trace in this region revealing a progressive loosening as it approaches the point where the chain joins with the αC domain in the chicken fibrinogen (or the highly repetitive structure in mammalian fibrinogens) (Figure 5). The very earliest targets for plasmin are known to be situated in this region of the α chain (*36*).

Even at 2.7 Å resolution, the electron density corresponding to the flexible αC domains, which encompass residues α220−491 (chicken numbering), is too weak for tracing the individual chain paths. Considerations of crystal packing, however, make it possible to rule out some locations for these 25 kDa αC domains. Although some workers have suggested that the αC domains must interact in an intramolecular fashion (*37*), in the crystal the only possible interactions seem to be between αC domains of adjacent molecules (Figure 2).

There have been conflicting views about how much structure the αC domains may have, even though most parties

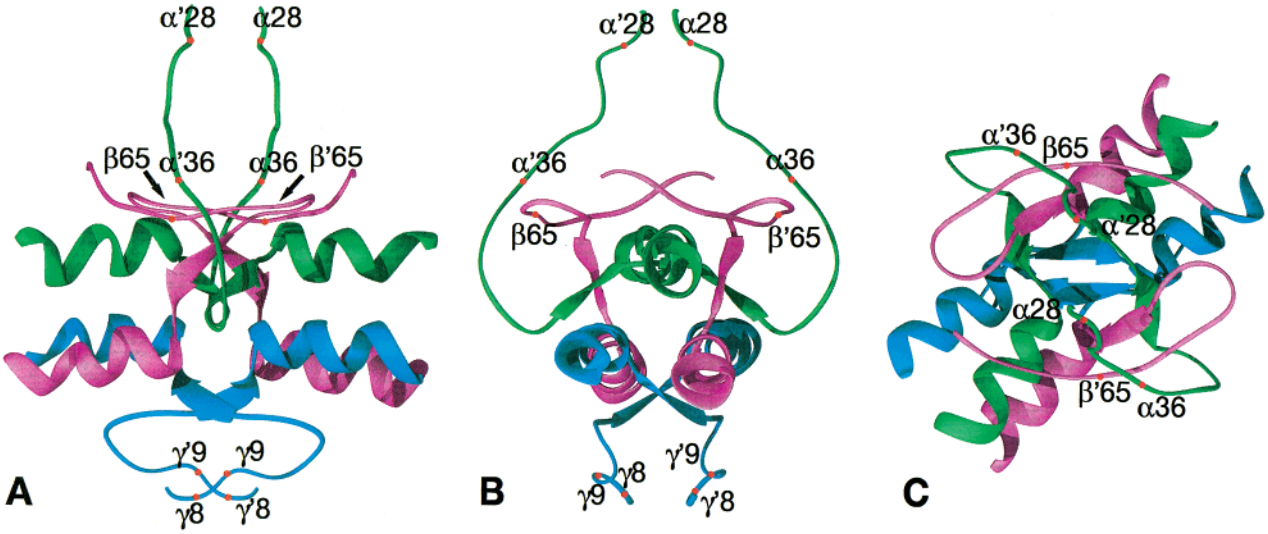

FIGURE 4: Three different views of a ribbon model of the central domain showing association of two halves by three short β sheets and interdigitations of chains from opposite sides (α chains, green; β chains, magenta; γ chains, blue). The $\gamma-\gamma$ bow tie is on the dorsal side of the molecule; the α and β chain amino-terminal sections both emerge from the ventral side.

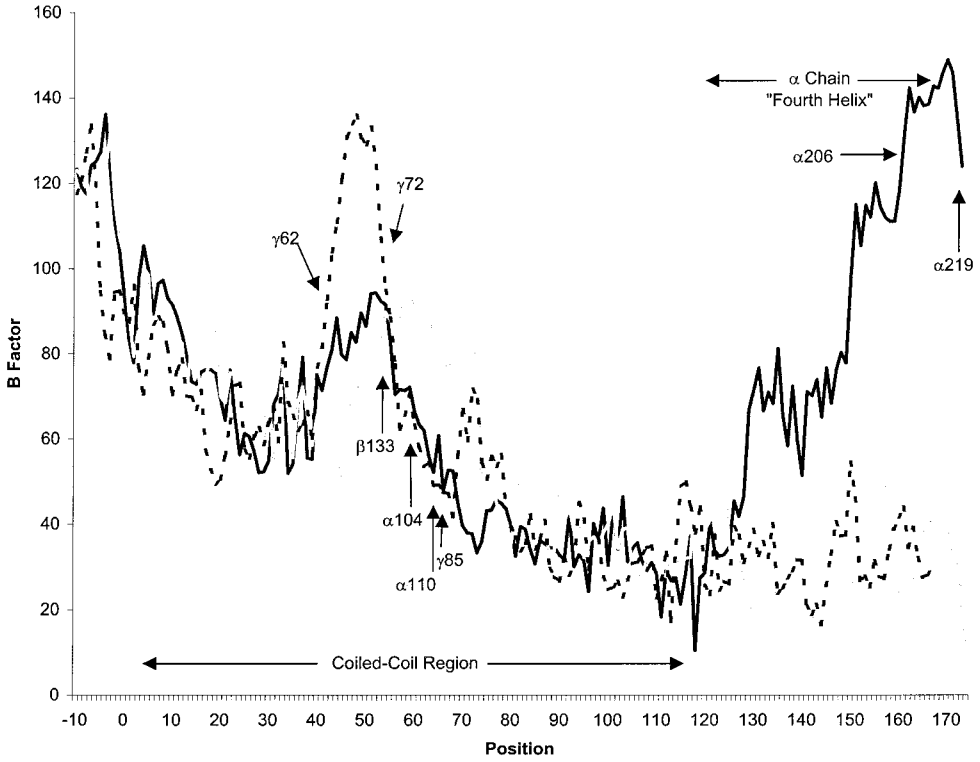

FIGURE 5: Plot of *B*-factors (temperature factors) by residue in the α (black), β (gray), and γ (dashed) chains of chicken fibrinogen in the regions between the disulfide rings and ~80 residues beyond (α49−α250, β80−β280, and γ23−γ225). The ABC side of the model is shown; the DEF side has slightly higher *B*-factors on average. Known plasmin attack points are denoted with arrows.

are in agreement that they are flexibly attached. The arguments against a compact domainal structure center around the extreme changes in length and sequence from species to species, as well as the rapid destruction of these regions by many proteases, including plasmin (*1*). On the other hand, calorimetry, especially in the case of bovine fibrinogen, has not only detected some indication of structure but also provided evidence that the domains interact with each other (*38*). These latter observations are thought to agree with electron microscopy studies which have reported an increased mass in the central region of fibrinogen over and beyond the contribution of the amino-terminal segments (*39*, *40*).

In the end, the X-ray data confirm the general mobility of the αC domain but do not resolve the matter of a structured domain. The data do not provide evidence for any preponderance of extra mass in the central region, crystal packing considerations and the exclusion principle showing that much of the central volume in the crystal is occupied by parts of other molecules. The X-ray structure is consistent with early fluorescence polarization reports of fibrinogen possessing

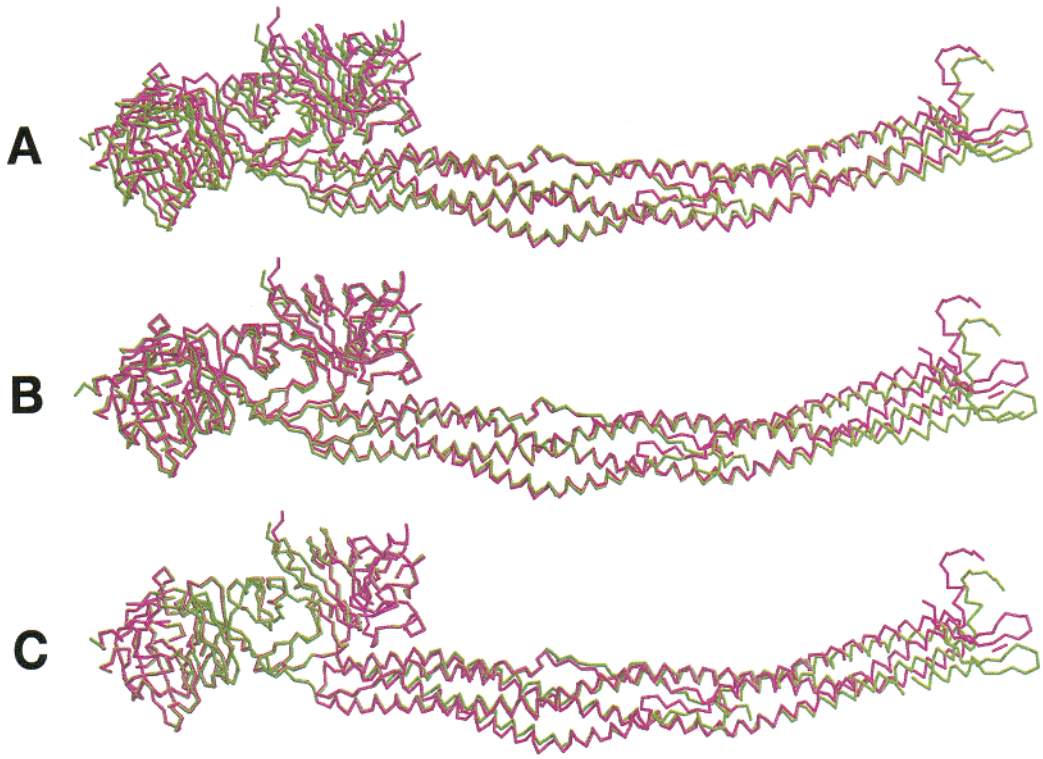

FIGURE 6: Three different rotational superpositions of one-half of chicken fibrinogen on the other half. In each case, the DEF half (green) of a model of chicken fibrinogen was superimposed by least-squares fitting on the ABC half (magenta) of a copy of the model. (A) Superposition of full-length coiled coils (rms for 340 fitted residues = 1.703). (B) Superposition of distal halves of coiled regions only (rms for 153 fitted residues = 0.696). (C) Superposition of the βC and γC domains (rms for 502 fitted residues = 0.437).

segmental flexibility (*41*, *42*), in contrast to later studies describing a rigid molecule (*43*, *44*).

DISCUSSION

Each half of the chicken molecule is composed of 1364 amino acid residues. Of these, approximately 700 are in the fragment D region, for which high-resolution structures are available for the human equivalent (*9*). The model for each half of the native chicken molecule contains an additional 280 residues from the central domain and the remainder of the coiled coil. As such, almost 30% of the residues are missing (Table 1), mostly from the αC domain (272 residues), but also the amino-terminal segments of the three chains (96 residues all told) and the γ chain carboxyl-terminal segment (16 residues). The mobility of these regions reflects idiosyncratic functional requirements, as well as a need for plasticity in the fibrin clot.

Comparison of Chicken and Mammalian Fibrinogens. All vertebrate fibrinogens follow a common plan, and it is clear that most of the features observed in the chicken fibrinogen are representative. Overall, chicken fibrinogen β and γ chains are 65−68% identical with their mammalian counterparts; there are no significant structural differences apparent in the mainframe regions available for comparison. In the case of α chains, the obvious sequence homology between chicken and mammals extends to human residue α245, at which point the 13-residue repeats begin in mammals; the sequence homology resumes at human residue α395.

The sequence resemblances are strongest in the globular regions. The amino acid sequences of the βC and γC domains from chicken and human fibrinogens are 78 and 80% identical, respectively. Superposition of the βC and γC domains from chicken fibrinogen on their human counterparts gave rms values of 0.57 (260 residues compared) and 0.91 (251 residues compared), respectively. The only notable structural differences observed are on loops, one in the β chain between residues β280 and β282 and another on the γ chain between residues γ357 and γ361. The key residues for binding the A and B knobs, including γGln329, γAsp330, γAsp364, βGlu397, βAsp398, and βAsp422, retain their exact three-dimensional positions, as do the key D−D interfacial residues, including γArg275, γTyr280, and γSer300. The carbohydrate cluster at βAsn364 is obvious on both sides of the molecule, as are calcium atoms in both the γC and βC domains.

Finally, we should note that although chicken fibrinogen binds the synthetic peptide Gly-His-Arg-Pro-amide, a surrogate of mammalian B knobs, the β chain of chicken fibrin ends with the sequence Ala-His-Arg-Pro (*45*). The strong sequence and structural resemblance between chicken and mammalian fibrinogens in the vicinity of the β chain hole is in accord with the observation that the chicken protein binds GHRPam perfectly well (Figure 7). The presence of the terminal alanine in chicken fibrinogen β chains was verified by PCR and DNA sequencing.

Thrombin Attachment and Flexibly Positioned Targets. Finding the exact location where thrombin binds fibrinogen during the release of fibrinopeptides remains a highly coveted goal. Thrombin differs from many serine proteases in that the primary binding site for its principal substrate (fibrinogen) is distinctly separate from the catalytic site (*46*). The exosite is composed of a constellation of positively charged side chains and binds negatively charged moieties such as hirudin. A secondary binding site on thrombin binds to the carboxyl

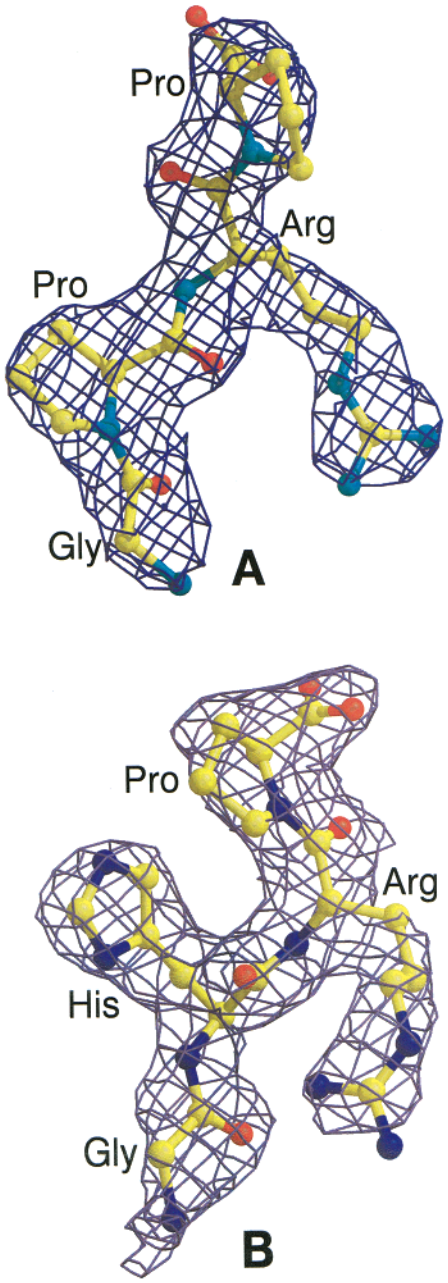

FIGURE 7: Electron density map ($3F_o - 2F_c$) for bound peptide ligands in chicken fibrinogen. The peptides were not included in the F_c calculation. (A) Gly-Pro-Arg-Pro-amide data calculated at 1.5σ. (B) Gly-His-Arg-Pro-amide data calculated at 1.0σ.

portions of fibrinopeptides and is adjacent to the catalytic site (*47*).

Biochemical findings (*48*) indicate that the site on fibrinogen for binding to the thrombin exosite is situated somewhere between residues αCys28 and αCys45. On the other hand, the only known variant human fibrinogens with an impaired ability to bind thrombin have their defects in the β chain. For example, fibrinogen New York (*49*) lacks the segment of residues β9−β72, and fibrinogen Naples (*50*) has only the subtle βAla68 to βThr68 substitution. Genetically engineered fibrinogens with the βAla68 to βThr68 substitution exhibit greatly delayed release of both fibrinopeptides A and B (*51*).

Neither the α nor the β chain is particularly well conserved from species to species in this region (Figure 8), the chicken

human α (28-49)	. . . **C**K DSDWPF**C**SDEDWNYK**C**PSG**C**. . .
bovine α (31-52)	. . . **C**K ETGWPF**C**SDEDWNTK**C**PSG**C**. . .
chicken α (28-50)	. . . **C**KYEKNWPI**C**VDDDWGTK**C**PSG**C**. . .
lamprey α (21-42)	. . . **C**ASATA DL**C**VHGDWGRK**C**PNG**C**. . .
human β (58-80)	. . . KAPDAGG**C**LHADPDLGVL**C**PTG**C**. . .
bovine β (65-87)	. . . KPPDADG**C**LHADPDLGVL**C**PTG**C**. . .
chicken β (63-85)	. . . IYPDAGG**C**KHPLDELGVL**C**PTG**C**. . .
lamprey β (79-101)	. . . AIRDEGG**C**MLPESDLGVL**C**PTG**C**. . .
human γ (1-23)	YVATRDN**C**CILDERFGSY**C**PTT**C**. . .
bovine γ (1-23)	YVATRDN**C**CILDERFGSY**C**PTT**C**. . .
chicken γ (1-23)	YIATREN**C**CILDERFGSY**C**PTT**C**. . .
lamprey γ (1-23)	QVRDLKQ**C** SNDPEFGRY**C**PTT**C**. . .

FIGURE 8: Alignment of homologous sequences in the central domain distal to the first disulfide ring. Conserved cysteine residues are emboldened.

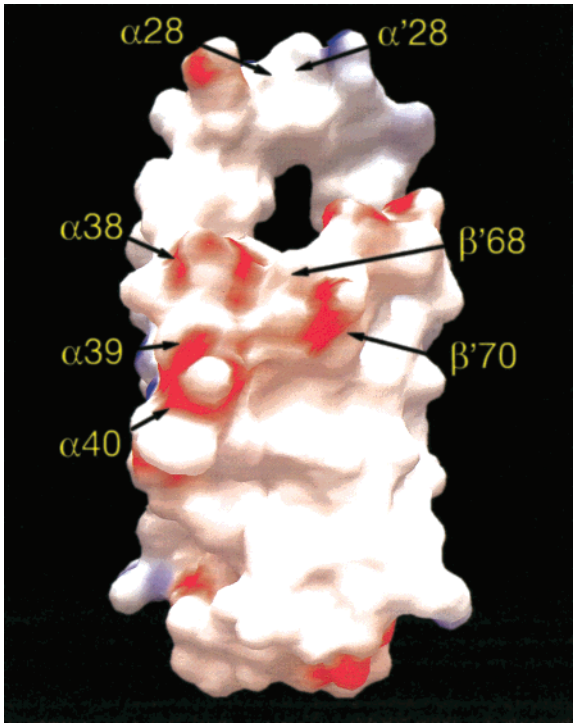

FIGURE 9: GRASP depiction (*30*) of the central domain from chicken fibrinogen showing the negatively charged platform that may bind to the thrombin exosite.

having a proline at the site of the fibrinogen Naples Ala → Thr change. Nonetheless, we examined the central domain for reasonable thrombin attachment sites. As it happens, there is a quite obvious negatively charged platform composed of the segments involving α38−α40 and β70 and β71 where the β chain protrudes through the α chain arch (Figure 9). Auspiciously, residue β68 is situated directly in the midst of the negatively charged cluster.

Other workers have proposed a model for thrombin binding to fibrinogen at the exosite in such a way that the α chain loops out before returning to bind at the fibrinopeptide binding site (*47*). As such, flexibility in this region seems not only reasonable but also obligatory; indeed, it may be what provides the advantage for having the attachment site spatially removed from the cleavage site. Consider the fact that the two α chains are bridled together at αCys28, a

location between the putative exosite binding region and the secondary fibrinopeptide binding site. Quite obviously, the two A fibrinopeptides must be more or less equally available for binding. As such, thrombin may not have to leave the binding site and return to remove the second fibrinopeptide A. This would be consistent with longstanding evidence that thrombin releases the second fibrinopeptide A many times faster than the first (*52*, *53*).

It is well-known that in mammalian fibrinogens the A fibrinopeptides are released much faster than are the B fibrinopeptides (*54*). The β chains are even less constrained than the α chains in this region, the thrombin-sensitive bonds being 50 residues away from the α36−β65 disulfide and 43 residues removed from the last residue positioned in the model (βPro60). As a consequence, the B knobs may be very widely separated. We have previously proposed that they are well positioned for a subsequent interaction with βC holes in the same pair of molecules being bridged by the A knobs of the same molecule (*55*). It may be that the β chain cleavage sites, flexibly situated and distant as they may be, can also be attacked from the strategically positioned thrombin once the A fibrinopeptides are removed. In any case, it is the flexible nature of the amino-terminal regions of the α and β chains that allows the coordinated release of the fibrinopeptides and facilitates the coincident exposure of pairs of knobs needed for bridging holes in neighboring molecules.

ACKNOWLEDGMENT

We are grateful to Marcia Riley for much technical assistance. We also thank George Rose for helpful comments and the staff at the Advanced Light Source at Lawrence Berkeley National Laboratory (Berkeley, CA) for their cooperation during our visit.

REFERENCES

1. Doolittle, R. F. (1973) *Adv. Protein Chem. 27*, 1−109.
2. Hall, C. E., and Slayter, H. S. (1959) *J. Biophys. Biochem. Cytol. 5*, 11−16.
3. Bailey, K., Astbury, W. T., and Rudall, K. M. (1943) *Nature 151*, 716−717.
4. Williams, R. C. (1981) *J. Mol. Biol. 150*, 399−408.
5. Rao, S. P. S., Poojary, M. D., Elliott, B. W., Jr., Melanson, L. A., Oriel, B., and Cohen, C. (1991) *J. Mol. Biol. 222*, 89−98.
6. Yee, V. C., Pratt, K. P., Cote, H. C., LeTrong, I., Chung, D. W., Davie, E. W., Stenkamp, R. E., and Teller, D. C. (1997) *Structure 5*, 125−138.
7. Pratt, K. P., Cote, H. C. F., Chung, D. W., Stenkamp, R. E., and Davie, E. W. (1997) *Proc. Natl. Acad. Sci. U.S.A. 94*, 7176−7181.
8. Spraggon, G., Everse, S., and Doolittle, R. F. (1997) *Nature 389*, 455−462.
9. Everse, S. J., Spraggon, G., Veerapandian, L., Riley, M., and Doolittle, R. F. (1998) *Biochemistry 37*, 8637−8642.
10. Everse, S. J., Spraggon, G., Veerapandian, L., and Doolittle R. F. (1999) *Biochemistry 38*, 2941−2946.
11. Brown, J. H., Volkmann, N., Jun, G., Henschen, A. H., and Cohen, C. (2000) *Proc. Natl. Acad. Sci. U.S.A. 97*, 85−90.
12. Murakawa, M., Okamura, T., Kamura, T., Shibuya, T., Harada, M., and Niho, Y. (1993) *Thromb. Haemostasis 69*, 351−360.
13. Doolittle, R. F., Watt, K. W. K., Cottrell, B. A., Strong, D. D., and Riley, M. (1979) *Nature 280*, 464−468.
14. Weissbach, L., and Grieninger, G. (1990) *Proc. Natl. Acad. Sci. U.S.A. 87*, 5198−5202.
15. Yang, Z., Mochalkin, I., Veerapandian, L., Riley M., and Doolittle, R. F. (2000) *Proc. Natl. Acad. Sci. U.S.A. 97*, 3907−3912.
16. Kuyas, C., Haeberli, A., Walder, P., and Straub, P. W. (1990) *Thromb. Haemostasis 63*, 439−444.
17. Deutsch, D. G., and Mertz, E. T. (1970) *Science 170*, 1095−1096.
18. Lin, T.-Y., and Timasheff, S. N. (1994) *Biochemistry 33*, 12695−12701.
19. Laudano, A. P., and Doolittle, R. F. (1978) *Proc. Natl. Acad. Sci. U.S.A. 75*, 3085−3089.
20. Otwinowski, Z., and Minor, W. (1997) *Methods Enzymol. 276*, 307−326.
21. Navaza, J. (1994) *Acta Crystallogr. A50*, 157−163.
22. Collaborative Computing Project Number 4 (1994) *Acta Crystallogr. D50*, 760−763.
23. Read, R. J. (1986) *Acta Crystallogr. A42*, 140−149.
24. Jones, T. A., Zou, J.-Y., Cowan, S. W., and Kjeldgaard, M. (1991) *Acta Crystallogr. A47*, 110−119.
25. Brunger, A. T., Adams, P. D., Clore, G. M., DeLano, W. L., Gros, P., Grosse-Kunstleve, R. W., Jiang, J.-S., Kuszewski, J., Nilges, M., Pannu, N. S., Read, R. J., Rice, L. M., Simonson, T., and Warren, G. L. (1998) *Acta Crystallogr. D54*, 905−921.
26. McRee, D. E. (1992) *J. Mol. Graphics 10*, 44−46.
27. Kraulis, P. J. (1991) *J. Appl. Crystallogr. 24*, 946−950.
28. Merritt, E. A., and Murphy, M. E. P. (1994) *Acta Crystallogr. D50*, 869−873.
29. Lawrence, M. C., and Bourke, P. (2000) *J. Appl. Crystallogr. 33*, 990−991.
30. Nicholls, A., Sharp, K., and Honig, B. (1991) *Proteins: Struct., Funct., Genet. 11*, 281−296.
31. Carson, M. (1997) *Methods Enzymol. 277*, 493−505.
32. Huang, S., Cao, Z., and Davie, E. W. (1993) *Biochem. Biophys. Res. Commun. 190*, 488−495.
33. Zhang, J.-Z., Kudryk, B., and Redman, C. M. (1993) *J. Biol. Chem. 268*, 11278−11282.
34. Doolittle, R. F., Cassman, K. G., Cottrell, B. A., Friezner, S. J., and Takagi, T. (1977) *Biochemistry 16*, 1710−1715.
35. Takagi, T., and Doolittle, R. F. (1975) *Biochemistry 14*, 940−946.
36. Takagi, T., and Doolittle, R. F. (1975) *Biochemistry 14*, 5149−5156.
37. Gorkun, O. V., Veklich, Y. I., Medved, L. V., Henschen, A. H., and Weisel, J. W. (1994) *Biochemistry 33*, 6986−6997.
38. Medved, L. V., Gorkun, O. V., and Privalov, P. L. (1984) *FEBS Lett. 160*, 291−295.
39. Wall, J., Hainfeld, L., Haschmeyer, R. H., and Mosesson, M. W. (1983) *Ann. N.Y. Acad. Sci. 408*, 164−179.
40. Erickson, H. P., and Fowler, W. E. (1983) *Ann. N.Y. Acad. Sci. 408*, 146−163.
41. Johnson, P., and Mihalyi, E. (1965) *Biochim. Biophys. Acta 102*, 476−486.
42. Hantgan, R. R. (1982) *Biochemistry 21*, 1821−1829.
43. Acuna, A. U., Gonzalez-Rodriguez, J., Lillo, M. P., and Razi Naqvi, K. (1987) *Biophys. Chem. 26*, 55−61.
44. Acuna, A. U., Gonzalez-Rodriguez, J., Lillo, M. P., and Razi Naqvi, K. (1987) *Biophys. Chem. 26*, 63−70.
45. Weissbach, L., Oddoux, C., Procyk, R., and Grieninger, G. (1991) *Biochemistry 30*, 3290−3294.
46. Fenton, J. W., Olson, T. A., Zabinski, M. B., and Wilner, G. D. (1988) *Biochemistry 27*, 7106−7112.
47. Stubbs, M. T., Oschkinat, H., Mayer, M., Huber, R., Angliker, H., Stone, S. R., and Bode, W. (1992) *Eur. J. Biochem. 206*, 187−195.
48. Binnie, C. G., and Lord, S. T. (1991) *Thromb. Haemostasis 65*, 165−168.
49. Liu, C. Y., Wallen, P., and Handley, D. A. (1986) in *Fibrinogen, Fibrin and Fibrinolysis* (Lane, D. A., Henschen,

A., and Jasani, M. K., Eds.) Vol. 4, pp 79−90, Walter de Gruyter and Co., Berlin.
50. Koopman, J., Haverkate, F., Lord, S. T., Grimbergen, J., and Manunucci, P. M. (1992) *J. Clin. Invest. 90*, 238−244.
51. Lord, S. T., Strickland, E., and Jaycock, E. (1996) *Biochemistry 35*, 2342−2348.
52. Landis, W. J., and Waugh, D. F. (1975) *Arch. Biochem. Biophys. 168*, 498−511.
53. Bale, M. D., Jamney, P. A., and Ferry, J. D. (1982) *Biopolymers 21*, 2265−2277.
54. Shainoff, J. R., and Page, I. (1960) *Circ. Res. 8*, 1013−1022.
55. Yang, Z., Mochalkin, I., and Doolittle, R. F. (2000) *Proc. Natl. Acad. Sci. U.S.A. 97*, 14156−14161.

BI011394P